

Formation of garnet clusters during polyphase metamorphism

David Floess and Lukas Baumgartner

Institute of Earth Sciences, University of Lausanne, 1015, Lausanne Switzerland

ABSTRACT

Pre-Alpine garnets of Variscan age from metapelitic basement units in Northern Italy were **strongly retrogressed** at near-surface conditions prior to Alpine **contact** metamorphism. The replacement by sheet silicates caused a significant volume increase during retrogression, producing pervasive fracturing. Up to several hundreds of angular fragments formed from each crystal. Electron backscatter diffraction analysis documents a maximum **misorientation of 22°** of some fragments as a result of local rotation during fracturing. New garnet growth is observed on the garnet fragments during contact metamorphic overprinting, resulting in **garnet clusters**. Frag-

ments can be identified due to calcium-rich domains. Fragment orientations were inherited, and only minor new nucleation occurred. These garnets develop features typically associated with **multiple nucleation models**, but here they reflect multiple metamorphic events. We propose that clusters can be indicative of multiple metamorphic events, which were separated by a period of intense retrograde alteration.

Terra Nova, 25, 144–150, 2013

Introduction

Garnet plays a central role in metamorphic thermobarometry and geochronology, as well as in kinetic, diffusion and recrystallization studies. It is a refractory mineral, which is capable of preserving prograde chemical zoning to temperatures in excess of 600 °C; garnet is ubiquitous in medium- to high-grade metamorphic rocks and its thermodynamics is well understood. Garnet progressively fractionates its 'nutrient' elements into its crystal structure, depleting the matrix (Hollister, 1966). Despite the fact that garnet can grow in disequilibrium with its surrounding matrix (Carlson and Denison, 1992; Skora *et al.*, 2006; Wilbur and Ague, 2006), its zoning can preserve information on the pressure, temperature and time evolution of the rock (e.g. Spear, 1993). Carlson and co-workers have argued that diffusion of Al in the matrix limits garnet growth (Carlson, 2002). In that case, almost no depletion haloes will be present for the divalent cations used to form garnet, and hence important equilibria, like Fe/Mg distribution between garnet and biotite, should yield equilibrium distribution coefficients (Baumgartner and Foster, 2005). Microstructures

showing **resorption** can be observed when a garnet is outside its P – T – X stability field, when **water infiltration** during the retrograde path occurs, or when garnet-consuming reactions progress on the prograde path. Growth and resorption can alternate, which leads to complex zoning patterns, in which newly grown garnet **anneals fractures** and embayments.

Nucleation and subsequent growth commonly lead to the formation of single, spatially separated crystals (e.g. Carlson and Denison, 1992; Kretz, 1993). Clustered nucleation is typically the result of **favorable nucleation** sites in a rock. In this light, the growth of clusters and aggregates of multiple crystals has fascinated researchers. Several studies investigated garnet aggregates or clusters (Daniel and Spear, 1998; Spiess *et al.*, 2001; Hirsch *et al.*, 2003; Whitney *et al.*, 2008). Some clusters show **preferential crystallographic orientations** of grains or domains, which require an explanation. Spiess *et al.* (2001) proposed that impingement and physical rotation of adjacent crystals during growth lead to preferred orientation of grains which initially nucleated with random orientation. This hypothesis is referred to here as multiple nucleation and coalescence. Spiess *et al.* (2007) also showed evidence for **epitaxial** growth of garnet in crenulated mica schists. This can result in clusters of garnets with the **same lattice orientation**.

Whitney *et al.* (2008) observed high-angle grain boundaries within

garnet clusters and proposed coalescences with increased likelihood for orientations, which have **low-energy** as some lattice sites coincide for these specific orientations. In either case, **closely** spaced nucleation is required. Nucleation on precursor phases provides preferential nucleation sites and common lattice orientations. Some features which can be interpreted as clustered nucleation were shown to result from **growth** of single garnets. Overgrowth of a precursor phase can produce a patchy chemical zoning mimicking clustered nucleation. For example, patchy Mn-zoning in garnets is explained by overgrowth of a Mn-rich mineral like ilmenite, chlorite or piemontite (Hirsch *et al.*, 2003), rather than by multiple nucleation. Finally, garnet clusters can form by **deformation**. Prior *et al.* (2000) report the formation of subgrains due to crystal plastic deformation of mantle garnets. The new subgrains have similar orientations to their parent crystal.

Common to all but the Prior *et al.* (2000) model is that the microstructural and microchemical observations are explained by a **single metamorphic event**. Here, we present an alternative model for the formation of garnet clusters, based on a **polymetamorphic** evolution. Garnet-bearing, amphibolite facies metapelites were exhumed and retrogressed near the surface and subsequently overprinted by contact metamorphism. This results in clusters which are comparable to the ones reported in the

Correspondence: David Floess, Institute of Earth Sciences, University of Lausanne, 1015 Lausanne, Switzerland. Tel.: +41 (0)21 692 44 52; fax: +41 (0) 21 692 43 05; e-mail: david.floess@unil.ch

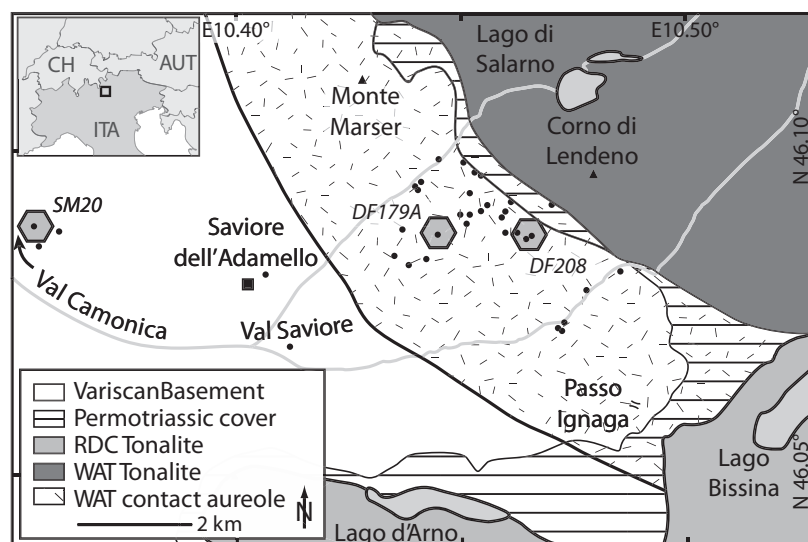


Fig. 1 Geological map of the western border of the Adamello batholith (modified after Callegari and Brack, 2002). The sample SM20 is located outside the contact aureole; samples DF179 and DF208 are located within the contact aureole of the Western Adamello tonalite (WAT). The WAT has an age of 38.26 Ma (Skopelitis *et al.*, 2010). Samples were not affected by the older (1 Ma) Re di Castello tonalite (RDC). Inset map shows the study area in the northern Italian Alps, Europe.

literature. A contact aureole represents an ideal natural laboratory. P – T – t paths are simple, the field geology well defined, and the same rock types can be followed from low metamorphic grade to high grade over a relatively short distance. In addition, the alteration or even obliteration of chemical zoning by diffusion is **minimized** due to the short thermal pulse.

Regional geology and sample locations

Garnet-bearing pelitic schists from the basement of the Southern Alps (Northern Italy) underwent Variscan metamorphism at amphibolite facies conditions (550–650 °C and 0.7–0.9 GPa at *c.* 330 Ma; Diella *et al.*, 1992). The basement was exhumed and cooled to near ambient temperatures prior to Permian sedimentation. The retrogression observed in garnets is most likely due to near-surface **alteration**, prior to Alpine metamorphism. The basement rocks experienced Anchizone metamorphism (250–300 °C) during the Late-Cretaceous Orobic deformation phase (Doglioni and Bosellini, 1987; Pennacchioni *et al.*, 2006), prior to the intrusion of the Tertiary Adamello batholith and contact metamorphism.

This study concentrated on metapelitic schists from the **contact aureole** of the Western Adamello Tonalite (WAT, Fig. 1), which is dated at 38.26 Ma (Skopelitis *et al.*, 2010). A strong thermal overprint from the approximately 1 Ma (Skopelitis *et al.*, 2010) older Re di Castello Tonalite, which intruded south of the study area, can be excluded since all samples **are far from** this latter contact. A total of 36 garnet-bearing schists were collected (Fig. 1, black dots). Three representative samples, one sample from **outside** (SM20) and two samples from **within** (DF179, DF208) the contact aureole, are discussed in detail here (Fig. 1, hexagons), to document the textural evolution as a function of distance from the intrusive contact. The extent of the contact aureole shown in Fig. 1 corresponds to the first occurrence of newly formed biotite (2200 m from contact).

Observations and results

Microstructure and microchemistry

Retrogressed amphibolite facies rocks from outside the contact aureole are mainly micaschists, phyllites and paragneisses, with minor granitic

orthogneisses. The rocks display a **strong alteration**. Mica-rich layers consist mainly of white mica, chlorite and some relict biotite (all generally <5 mm). The micas are oriented and define a pervasive foliation. The mica-rich layers are intercalated with quartz–feldspar-rich layers on a cm-scale. Fe-oxides and Fe-sulfides are a common feature in the mica-rich layers. Garnet occurs as **porphyroblasts** located exclusively **in or close** to the mica-rich domains of the rocks.

Garnets from outside the contact aureole (SM20) are highly **fractured** single crystals with a size of up to 10 mm. The fractures contain chlorite and clay minerals (Fig 2a and b). The major element zoning of this garnet is the result of Variscan metamorphism. The zoning is **truncated by the fractures** (Fig. 3b). These fractures form an angular but irregular mesh texture, dissecting the garnet into hundreds of fragments (Fig. 2a and b, Supplementary data S1). Fracture tips (Fig. 2b) propagate into garnet fragments ahead of the alteration zone. Initial (black arrow) and advanced (white arrow) stages of alteration and fracturing are present. Inclusions of ilmenite, pyrite, quartz and feldspar trace the Variscan foliation. Fractures are not influenced by inclusion trails. Garnet habits are generally well pre-

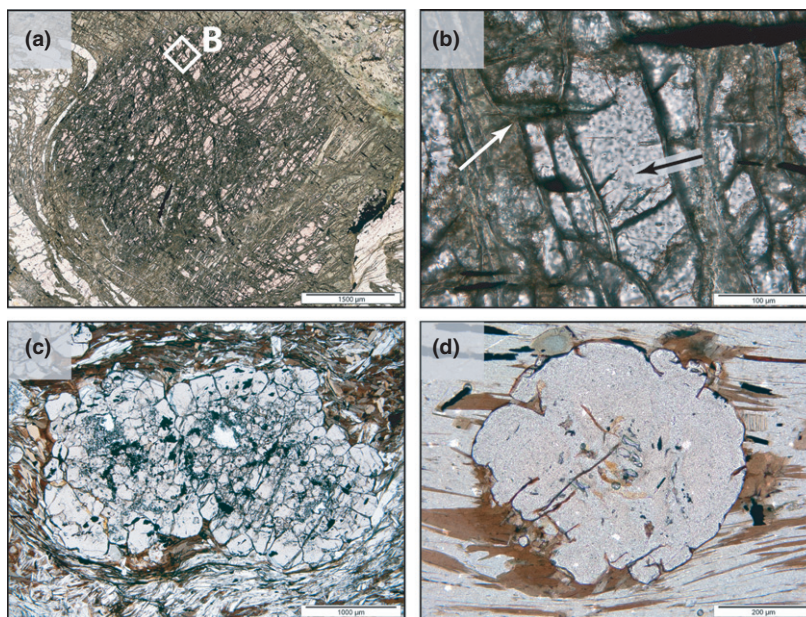


Fig. 2 Thin-section photomicrographs illustrating a retrogressed and fragmented Variscan garnet (a). A close-up of the retrogression microstructure in area B shows fracture tips at initial (black arrow) and advanced (white arrow) stages of alteration (b). Garnet clusters (c) and single crystals (d) occur in samples from the **contact aureole**. Garnet clusters consist of several hundred grains. Single crystals display no internal structure in thin section.

served even in crystals showing advanced retrogression.

Metapelites from within the contact aureole are the same rock type and experienced the same pre-intrusive history. Increased metamorphism results in the growth of andalusite and garnet (1700 m from contact). Muscovite breakdown, the sillimanite-in reaction and partial melting occur at a distance of 350 m from the contact. The sequence of assemblages corresponds essentially to the facies series 1c or 2a from Pattison and Tracy (1991). The main difference is the occurrence of andalusite down-grade of the muscovite–quartz breakdown reaction. This results in a widespread muscovite + quartz + andalusite + biotite + garnet + cordierite + plagioclase assemblage at medium grades. The isograd sequence limits the pressure during emplacement to ~ 2.5 kbar. The garnet overgrowth structures start at a temperature of ~ 500 °C, and are observed up to ~ 650 °C, at 350 m from the contact (Floess *et al.*, 2011). **Two types** of microstructures were observed: framboidal garnet clusters (Fig. 2c) and garnet single crystals (Fig. 2d). We use the adjective framboidal based on their resemblance to **raspberries** (French: framboise). Both

microstructures occur throughout the WAT contact aureole; clusters occur more frequently at medium metamorphic grades and become typically **less abundant towards the intrusive contact**, where single crystals are more abundant. Representative core–rim compositions are listed in the supplementary data table S2.

Framboidal garnet **clusters** measure up to 5 mm. They consist of several hundred individual grains (Figs 2c and 3f and i). The Ca X-ray maps show that most of the grains within a cluster have a **high-Ca core** (Fig. 3d and g). A low-Ca rim around the entire framboidal structure can occur resulting in the typical sub-idiomorphic habit of the clusters. Mn zonation is more **diffuse** and patchy, and generally **does not coincide** with Ca-rich domains. Ca-rich zones have a sharp boundary and are typically smaller than Mn-rich zones, especially towards the highest metamorphic grades.

A second type of microstructure consists of garnets of up to 3 mm in diameter, which looks like single crystals in thin section (Fig. 2d). Nevertheless, Ca and Mn element maps show **multiple islands and zones** (Fig. 3j and k). Irregular, sometimes amoeboid, dissolution of

the Variscan portion of the garnet (i.e. **fragments**) is documented by **abrupt changes** in garnet composition. Fractures are filled and **annealed** by low-Ca, medium-Mn garnet. Note the prominent fractures dissecting the concentric, Variscan zoning. Sharp gradients on the micron-scale mark the **transition** from Variscan to contact-metamorphic garnet. The overgrowth is not limited to the outside only, but occurs also in the center of the grain. Comparing the number of fragments in Fig. 3a and j documents that the intensity of fracturing and retrogression played an important role in determining the resulting microstructure (garnet crystal vs. cluster).

Crystallographic preferred orientations (CPO)

Pole figures obtained from electron backscatter diffraction (EBSD) analysis of altered Variscan garnets (Fig. 4a) show a strong common crystallographic orientation, with a density exceeding 45 times that of the uniform distribution (mud = multiple of the uniform distribution). **Some fragments show a misorientation of up to 22°.**

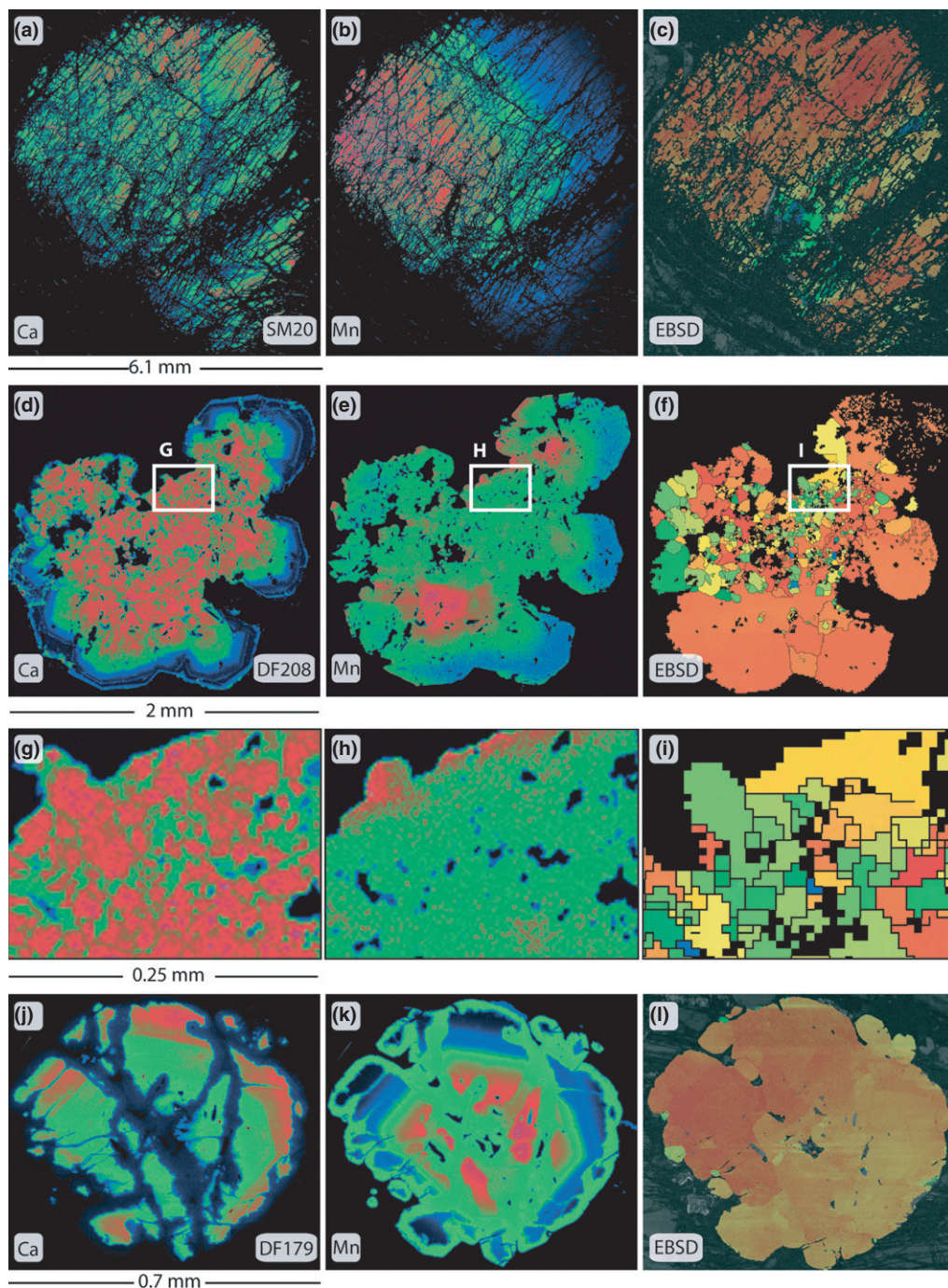


Fig. 3 Ca and Mn electron microprobe X-ray element maps (left two panels) and EBSD orientation maps (right panels) for partially altered Variscan garnet (a–c) and two samples from the Tertiary WAT contact aureole (d–l). a–c (Sample SM20, see micrograph Fig. 2a): Garnet zoning is visible despite the intense fracturing produced during low-*T* alteration of the garnet – no new garnet growth occurred. Fracturing was accompanied by significant rotation of individual fragments (up to 22°) indicated by the blue colors in the EBSD map. d–f (Sample DF208, areas G–I shown enlarged in g–i, respectively): Each Ca-rich zone in the garnet cluster represents a fragment of a Variscan garnet. The fragments have a low-Ca overgrowth and the cluster is partially surrounded by a rim, which is responsible for a sub-idiomorphic habit. Mn-concentrations are patchy and smoothed out by minor diffusion. Several hundred grains show a strong crystallographic preferred orientation: 64% of the crystals have a misorientation smaller than 20° (see supplementary data S3a and b). g–i (Sample DF208, see micrograph in Fig. 2d): Garnet shows fractures, which were filled by newly grown, low-Ca and medium-Mn garnet. The fractures dissect the prograde Variscan zoning. **No major crystallographic misfit** was observed for this grain. (Chemical maps: warm colors indicate higher concentration.)

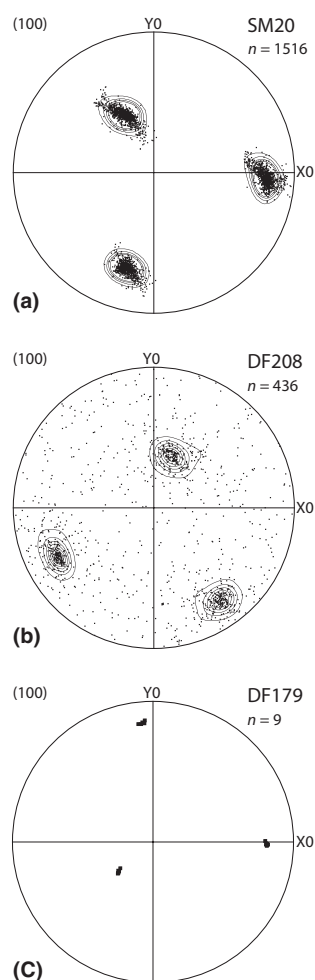


Fig. 4 Pole figures for the (100) lattice orientation (one point per subgrain) for samples shown in Fig. 3. The contour lines show the multiples of the uniform distribution (in mud units). All samples show strong clustering. Maximum values (mud) are 45 and 19 for samples SM20 and DF208, respectively. The distribution of grains in sample DF208 is clearly not random (see supplementary data S3b). Equal area projections, lower hemisphere, contour parameters = half width: 10°, cluster size: 5°, contour line spacing 2.5 mud).

The CPO of framboidal garnet clusters is **similar** to that of the altered Variscan garnet described above (Fig. 4a). A strong CPO was obtained and is shown in the contoured pole figures (Fig. 4b, mud >19). Most crystals within a cluster show only a **small misorientation**. EBSD orientation maps of the clusters reveal a rotation of up to 46°, but 64% of the analysed crystals

have a lattice misfit of <20° (see Supplementary material S3a). The misorientation angle histogram (see Supplementary material S3b) shows clearly that the grains within a cluster are **not oriented randomly**. Most grains with Ca-rich cores show a small crystallographic misfit (<20°). Some grains with **larger misfits** show Ca-cores, others do not. This might indicate nucleation of some new grains, or, alternatively, that the thin section did not intersect the Ca-rich core. The outermost part of the garnet was newly grown as documented by the absence of Ca-peaks. The rim shows a radial pattern of slightly misaligned crystals.

The EBSD map of a garnet appearing as a single crystal from sample DF179 (Fig. 3l) shows **minor misorientations** of the individual fragments. In fact, many fragments have the **same orientation** as their neighbors and the maximum misfit is 3°. This is shown in Fig. 4c, where the poles are very tightly clustered.

Discussion and conclusion

Alteration

Garnets from the basement of the Southern Alps were strongly **altered** after the amphibolite facies Variscan event. This retrogression caused a significant **volume increase** during garnet decomposition due to hydration. The stress generated by the volume increase led to additional fracturing, which in turn enhanced the **retrogression rates**. These observations are similar to results from numerical models (Jamveit *et al.*, 2008; Ryne *et al.*, 2008), which quantify the effect of fracturing due to volume-increasing hydration reactions. Their mechanical model uses a generic reaction leading to a volume increase. The pressure generates fractures in the brittle crystal, which results in a fracture network. Characteristic for such networks are incipient fractures, **filled with alteration** phases, but dead-end, as seen in our study in garnets (Fig. 2b). The models are applied to mafic rocks to investigate the processes behind weathering and the interaction of mechanical and chemical disintegration. Although these numerical models are restricted to rock fracturing

during retrogressive processes, grain-fracturing shows similar fragment shapes and fracture junction angles (Iyer *et al.*, 2008; Plümper *et al.*, 2012). A comparison of the above model results with the fracturing pattern observed in the fragmented Variscan garnets of the basement schists **shows striking similarities** (e.g. fracture tips in non-reacted fragments in Fig. 2b). Therefore we suggest that fracturing due to **volume increase at near-surface conditions** was an important component of retrogression. Nevertheless, we cannot exclude the possibility that some of the fractures originate from **tectonic stress** (Trepmann and Stöckhert, 2002). Our observations suggest that a rotational component during fracturing and/or retrogression is **present**, even for the alteration of such homogeneous, isotropic materials as the studied garnets. In such cases, the rotational component should be integrated in future models. We suggest that the irregular, **network-like** mesh textures presented in this study resulted from **hydration-induced fracturing** (Jamveit *et al.*, 2008; Plümper *et al.*, 2012) rather than tectonic stresses, though more detailed studies are needed.

Contact metamorphic overgrowth

The retrogressed garnet-bearing rocks underwent contact metamorphism subsequent to the fracturing process. Typical microstructures observed are (i) framboidal garnet clusters and (ii) garnets appearing as single crystals. We interpret these textural differences as a combination of (i) the **intensity of fracturing** of the pre-existing garnets during retrogression and (ii) the result of **enhanced recrystallization** at higher *T* closer to the contact. An intense fracturing of Variscan garnets results in **complex** framboidal microstructures, whereas weakly altered grains form **simple** microstructures (single crystals or aggregates of a few crystals). Recrystallization at elevated *T* **decreases** the misfit of orientation, and diffusion **reduces** gradients in chemistry. Pronounced Ca maxima are inherited from pre-existing garnet fragments. Garnet overgrowths due to the contact metamorphic thermal overprint are Ca-poor (low-*P*,

2.5 kbar). Detailed examination of the newly grown garnet sometimes shows irregular zoning, most evident in Mn concentration. The replacement of retrograde minerals containing varying amounts of Mn can explain such variations. This supports the results of Hirsch *et al.* (2003), who attributed a very short length of equilibration to Mn in garnet-bearing metapelites from the Harpswell Neck, Maine. On the other hand, our observations of Mn-zoning of high-grade samples suggest that Mn mobility increases substantially, both inside and outside, the garnet crystal. Hence, we confirm that Ca represents a better marker for the examination of growth microstructures than Mn, Mg and Fe.

Mineral orientations within the framboidal garnets (Fig. 4b) are quite constant. This is due to the fact that most of the garnet fragments were only rotated by minor amounts during retrogression, and new garnet formed homoepitaxial overgrowth. Hence, we interpret the common mineral orientations as being inherited from fragments, rather than clustered nucleation. The observed large misfit for some grains (Fig. 4b) is likely the result of large rotation during retrogression in peripheral areas of the garnet crystal or – for grains without Ca-rich domains – due to nucleation of new crystals. Some nucleation is supported by the observation that a few crystals without a Ca-peak do have a Mn-peak, which is typical for new nucleation and growth. However, we have no indication of substantial rotation upon impingement during growth as proposed by Spiess *et al.* (2001).

Examples from other geodynamic settings

Similar microstructures and chemical zoning patterns have been reported from a broad variety of metamorphic terranes: the Italian Alps (Spiess *et al.*, 2001), the North Cascades, USA (Whitney and Seaton, 2010) and the Carpathians, Romania (Săbău *et al.*, 2006), for example. Spiess *et al.* (2001) envisage random nucleation, followed by growth and rotation due to impingement of the garnet grains, which causes an arbitrary rotation of single grains until subdomains with

similar orientation develop. Continuous rotation of the subdomains further decreases the lattice misfit of the cluster and the result is a strong preferred orientation. The individual grains within a cluster show clear Ca peaks and a strong preferred orientation within a cluster was reported. The clusters are elongated (aspect ratio 2 : 1).

Some garnet clusters presented in the study of Whitney and Seaton (2010) show similarities to the ones presented in our study, in terms of the appearance of clusters in thin section (North Cascades – Fig. 8a, Santander Massif – Fig. 10a, c and e), their microchemistry (North Cascades – Fig. 8b, Harpswell Neck – Fig. 4c) and microstructures (Harpswell Neck, Fig. 4e). Nevertheless, a direct comparison is only possible to a limited extent because of missing information on either chemistry or orientation for some types of clusters.

The garnets presented by Săbău *et al.* (2006) are single, euhedral to subhedral crystals. The chemical maps reveal several isolated zones with distinct differences in divalent cation concentration within a crystal. Multiple nucleation and growth by coalescence is used to explain their formation. Some of these zones have fragment-like forms and might result from a fracturing/overgrowth process. EBSD maps are needed for further discussion about their formation.

In conclusion, we suggest that the formation of clusters with low-angle misorientations can potentially be explained by our mechanism and that this might be a more common process. We infer that the number of grains (fragments) within a cluster depends on the intensity of fracturing. Therefore, if a cluster forms due to a fragmentation–overgrowth process, the number of grains within a cluster can vary strongly. The absolute concentration of divalent cations (Ca, Fe, Mg and Mn) will be influenced by the initial fragment composition (cores), the new *P–T* conditions under which the overgrowth forms, as well as the accessible whole-rock chemistry for the overgrowth. It is evident that not all of the fragments necessarily need to have the same composition, especially if they originate from an initially zoned garnet.

The formation of the clusters due to crystal plastic deformation (i.e. subgrain formation reported by Prior *et al.*, 2002; Bestmann *et al.*, 2008 and Storey and Prior, 2005) can be excluded since no intense intrusion-related deformation of the studied basement rocks is observed.

Summary

The comparison of garnet-bearing basement rocks from within and outside a contact metamorphic aureole allows us to establish an alternative model for the formation of clustered garnet microstructures. Fractured Variscan garnets from outside the contact aureole are strongly retrogressed and replaced by sheet silicates. The observed mesh texture and fracture tips in the fractured crystals suggest near-surface alteration. The same generation of garnet – where affected by the Alpine contact metamorphism – developed distinct overgrowth rims. This results in formation of clusters, where orientations are inherited from pre-existing fragments. Although generally associated with multiple nucleation and coalescence models, these garnet clusters formed by a fragmentation and overgrowth process. This mechanism might also serve to explain garnet cluster formation in other geodynamic settings.

Acknowledgements

We thank Tom Foster, Pierre Vonlanthen and Othmar Müntener for fruitful discussions and comments. We thank Bernardo Cesare and two anonymous reviewers for constructive comments, which significantly improved the manuscript. This research was funded by the Swiss National Science Foundation grant 'ProDoc Adamello' PDFMP2-123081 and grant 200020_125261. We thank the 'Parco dell'Adamello' for giving permission to collect samples.

References

- Baumgartner, L.P. and Foster, C.T., 2005. Application of a continuum diffusion model to metamorphic crystallization. *Suppl. Geochim. Cosmochim. Acta*, **69**, A403.
- Bestmann, M., Habler, G., Heidelbach, F. and Thoeni, M., 2008. Dynamic recrystallization of garnet and related diffusion processes. *J. Struc. Geol.*, **30**, 777–790.

- Callegari, E. and Brack, P., 2002. Geological map of the Tertiary Adamello batholith (Northern Italy) – Explanatory notes and legend. *Sci. Geol. Mem.*, **54**, 19–49.
- Carlson, W.D., 2002. Scales of disequilibrium and rates of equilibrium during metamorphism. *Am. Mineral.*, **87**, 185–204.
- Carlson, W.D. and Denison, C., 1992. Mechanisms of porphyroblast crystallization: results from high-resolution computed X-ray tomography. *Science*, **257**, 1236–1239.
- Daniel, C.G. and Spear, F.S., 1998. Three-dimensional patterns of garnet nucleation and growth. *Geology*, **26**, 503–506.
- Diella, V., Spalla, M.I. and Tunesi, A., 1992. Contrasting thermomechanical evolutions in the Southalpine metamorphic basement of the Orobic Alps (Central Alps, Italy). *J. Metamorph. Geol.*, **10**, 203–219.
- Doglioni, C. and Bosellini, A., 1987. Eoalpine and mesoalpine tectonics in the Southern Alps. *Geol. Rundsch.*, **76**, 735–754.
- Floess, D., Baumgartner, L., Vonlanthen, P. and Brack, P., 2011. *Emplacement of the Western Adamello pluton, Southern Alps – Italy*. AGU fall meeting, San Francisco.
- Hirsch, D.M., Prior, D.J. and Carlson, W.D., 2003. An overgrowth model to explain multiple, dispersed high-Mn regions in the cores of garnet porphyroblasts. *Am. Mineral.*, **88**, 131–141.
- Hollister, L.S., 1966. Garnet zoning: an interpretation based on the Rayleigh fractionation model. *Science*, **154**, 1647–1651.
- Iyer, K., Jamtveit, B., Mathiesen, J., Mälthe-Sørenssen, A. and Feder, J., 2008. Reaction-assisted hierarchical fracturing during serpentinization. *Earth Planet. Sci. Lett.*, **267**, 503–516.
- Jamtveit, B., Mälthe-Sørenssen, A. and Kostenko, O., 2008. Reaction enhanced permeability during retrogressive metamorphism. *Earth Planet. Sci. Lett.*, **267**, 620–627.
- Kretz, R., 1993. A garnet population in Yellowknife schist, Canada. *J. Metamorph. Geol.*, **11**, 101–120.
- Pattison, D. and Tracy, R., 1991. Phase equilibria and thermobarometry of metapelites. *Rev. Mineral. Geochem.*, **26**, 105–120.
- Pennacchioni, G., Di Toro, G., Brack, P., Menegon, L. and Villa, I.M., 2006. Brittle-ductile-brittle deformation during cooling of tonalite (Adamello, Southern Italian Alps). *Tectonophysics*, **427**, 171–197.
- Plümpner, O., Ryne, A., Magrasó, A. and Jamtveit, B., 2012. The interface-scale mechanism of reaction-induced fracturing during serpentinization. *Geology*, **40**, 1103–1106.
- Prior, D., Wheeler, J., Brenker, F., Harte, B. and Matthews, M., 2000. Crystal plasticity of natural garnet: new microstructural evidence. *Geology*, **28**, 1003–1006.
- Prior, D., Wheeler, J., Peruzzo, L., Spiess, R. and Storey, C., 2002. Some garnet microstructures: an illustration of the potential of orientation maps and misorientation analysis in microstructural studies. *J. Struct. Geol.*, **24**, 999–1011.
- Ryne, A., Jamtveit, B., Mathiesen, J. and Mälthe-Sørenssen, A., 2008. Controls on rock weathering rates by reaction-induced hierarchical fracturing. *Earth Planet. Sci. Lett.*, **275**, 364–369.
- Săbău, G., Negulescu, E. and Massonne, H.-J., 2006. Chemical zonation and relative timing of growth sections in garnets from eclogites of the Leaota Massif. *South Carpath. Mineral. Mag.*, **70**, 655–667.
- Skopelitis, A., Schaltegger, U., Ulianov, A. and Brack, P., 2010. The Adamello batholith (Italy): a fossil magma chamber or accumulation of magma pulses? Swiss Geoscience Meeting 2010: Fribourg – CH.
- Skora, S., Baumgartner, L., Mahlen, N., Johnson, C., Pilet, S. and Hellebrand, E., 2006. Diffusion-limited REE uptake by eclogite garnets and its consequences for Lu–Hf and Sm–Nd geochronology. *Contrib. Mineral. Petrol.*, **152**, 703–720.
- Spear, F.S., 1993. *Metamorphic Phase Equilibria and Pressure-Temperature-Time Paths*, 799 p. Mineralogical Society of America, Washington, D. C.
- Spiess, R., Peruzzo, L., Prior, D.J. and Wheeler, J., 2001. Development of garnet porphyroblasts by multiple nucleation, coalescence and boundary misorientation-driven rotations. *J. Metamorph. Geol.*, **19**, 269–290.
- Spiess, R., Groppo, C. and Compagnoni, R., 2007. When epitaxy controls garnet growth. *J. Metamorph. Geol.*, **25**, 439–450.
- Storey, C.D. and Prior, D.J., 2005. Plastic deformation and recrystallization of garnet: a mechanism to facilitate diffusion creep. *J. Petrol.*, **46**, 2593–2613.
- Trepmann, C.A. and Stöckhert, B., 2002. Cataclastic deformation of garnet: a record of synseismic loading and postseismic creep. *J. Struct. Geol.*, **24**, 1845–1856.
- Whitney, D. and Seaton, N., 2010. Garnet polycrystals and the significance of clustered crystallization. *Contrib. Mineral. Petrol.*, **160**, 591–607.
- Whitney, D.L., Goergen, E.T., Ketcham, R.A. and Kunze, K., 2008. Formation of garnet polycrystals during metamorphic crystallization. *J. Metamorph. Geol.*, **26**, 365–383.
- Wilbur, D.E. and Ague, J.J., 2006. Chemical disequilibrium during garnet growth: Monte Carlo simulations of natural crystal morphologies. *Geology*, **34**, 689–692.

Received 1 February 2012; revised version accepted 25 October 2012

Supporting Information

Additional Supporting Information may be found in the online version of this article:

Data S1. Photomicrograph mesh texture.

Data S2. Representative electron microprobe analyses.

Data S3. EBSD data.